

# Cracking mechanisms of clay-based and GCC-based coatings

Peter Rättö, Joanna Hornatowska, Xiao Changhong and Osamu Terasaki

**KEYWORDS:** Binder, Coating, Cracking, Creasing, Folding, Pigment, Latex, Starch, Electron microscopy

**SUMMARY:** A new method to produce SEM cross sections was used to analyze coated and creased samples. It was found that the binder surrounded the smaller particles leaving the large pores around the larger pigment particles. Consequently, cracks would propagate next to the large particles, and at least one crack area also showed a clear pigment surface, indicating an adhesive failure between the binder and the pigment particles.

GCC and clay showed different cracking directions. GCC-based coatings showed cracks that had been initiated at the surface of the coating layer and then went through the thickness direction of the coating layer. The clay-based coatings on the other hand showed cracks that could be initiated anywhere in the thickness direction in the coating layer and then continued at an angle in the thickness direction. The cracking behaviour of the clay based coatings was probably due to anisotropic mechanical properties combined with shear stresses or out-of-plane tensile stresses during creasing.

**ADDRESSES OF THE AUTHORS:** Peter Rättö (peter.ratto@innventia.com) and Joanna Hornatowska (joanna.hornatowska@innventia.com): INNVENTIA AB, Box 5604, SE-114 86 Stockholm, Sweden. Xiao Changhong (changhong.xiao@mmk.su.se) Stockholm University, Department of Materials and Environmental Chemistry, SE-106 91 Stockholm, Sweden and Osamu Terasaki (terasaki@mmk.su.se): Stockholm University, Department of Materials and Environmental Chemistry, SE-106 91 Stockholm, Sweden and EWS (WCU), Korea Advanced Institute of Science and Technology (KAIST) Yuseong Gu, Daejeon 305-701 (Republic of Korea).

**Corresponding author: Peter Rättö**

Paper and board are coated in order to improve brightness, gloss and print quality. During the coating operation, a suspension consisting of mainly pigment and binder is applied onto the paper surface leaving a porous stiff layer after consolidation and drying. After the printing operation, publication papers such as LWC are subjected to folding and boards are usually subjected to creasing. Both these operations impose large strains on the coating layer, which might result in cracking of the coating layer. Cracking causes a problem with the visual appearance of coated paper and board, but might also reduce the tensile strength of the printed products to the point where the paper breaks at the folding line.

Strength loss of coated publication papers has been the subject of numerous papers (Colley 1982a;

1982b, Guyot et al. 1992, Jopson, Towers 1995) using a method of comparing the tensile strength before and after folding (Colley 1982a). Even if the cracks usually develop in the coating layer, the prevailing view is that the base paper has a great influence on the cracking tendency of coated papers. Jopson and Towers (1995) compared different combinations of base papers and coating layers and found the relationship between the base paper properties and the coating layer properties influenced the point of crack initiation. Thus, for example, a weak base paper combined with a stiff coating layer would result in failure within the base stock. Barbier et al. (2004) used numerical simulation and suggested that the deformation of the coating layer is determined by the thicker paper and the stress was highest away from the symmetry line. Board is even thicker than paper, but the in-plane strains of the surface layers are usually reduced due to delamination during creasing. Dia and Canella (2008) observed a decrease in crease stiffness of board at the point of delamination and numerical simulation of creasing performed by Nygård et al. (2009) indicate that creasing of board result in large out-of-plane tensile stresses and shear stresses. By measuring the crack area of creased samples, Rättö and Hornatowska (2010b) suggested that the loading case and mechanical properties of the coating layer might have an influence of the failure process. Shear forces combined with weak shear strength of clay based coating layers resulted in delamination rather than cracking through the thickness direction of the coating layer.

Barbier et al. (2002) also observed that cracking of the coating layer occurred on a very fast time scale, which implies that a stress-based failure criterion should be relevant (Barbier et al. 2002). This was partly confirmed by Rättö and Hornatowska (2010a) who studied the dynamical process of failure of coating layers during uni-axial tensile loading. Cracking of unsupported coating layers occurred momentarily and showed no energy release prior or during failure. Since cracking of the coating layer seemed to be initiated by flaws within the coating layer, they suggested that a failure of the coating layer could be described by a statistical approach.

The in-plane elastic and viscoelastic properties of coating layers have been widely studied (Lepoutre, Rigdahl 1989, Kan et al. 1997, Prall et al. 2000, Wikström et al. 2000, Toivakka, Bousfield 2001,

Rättö 2004, Husband et al. 2007, Alam et al. 2007). Flat pigments such as clay improve the in-plane tensile stiffness and strength compared to round pigments like GCC, due to reinforcement in the loading direction (Lepoutre, Rigdahl 1989, Husband et al. 2007). This reinforcement is improved with the flatness of the pigment particles (Husband et al. 2009) but is usually at the expense of out-of-plane properties. Numerical simulations by Rättö (2006) have also suggested that the bending and shear stiffness of the coating layer might be more complex than described by one-dimensional beam bending.

Several publications have also shown that the viscoelastic properties of the binder and the binder content will have a great influence on the viscoelastic properties of the coating layer (Kan et al. 1997, Prall et al. 2000, Toivakka, Bousfield 2001, Wikström et al. 2000). The works by Salminen et al. (2008a; 2008b) and Alam et al. (2009) also suggest that the mechanical properties of coating layers can be optimised in terms of cost, bending stiffness and cracking resistance with the use of multiple coating layers and buffer cracking zones.

The way the binder binds the particles together might also influence the mechanical properties quite considerably. Alam and Toivakka (2010) used micromechanical simulations to investigate how adhesive and cohesive failure mechanisms, respectively, affect the mechanical properties. An increased amount of adhesive failures (failure in the interface between the pigment particle and the binder) would give a more brittle behaviour compared to a higher amount of cohesive failures (failures within the latex bridges). The investigation of Husband et al. (2007) suggested that the binder would only exist as bonded to the particles at lower binder contents while segments of free binder would exist at higher binder contents. The strain at break would also increase quite rapidly with the binder content when segments of free binder are available. By applying new microscopic techniques, Ström et al. (2010), were able to show that the binder would gather around the small particles leaving few, but large, pores near the larger particles. Increased binder content would first fill the smaller pores around the small particles before filling out the larger pores.

The work presented here is a continuation of two previous publications (Rättö, Hornatowska 2010a; 2010b), where new methods were used to characterize surface cracks of coated papers both statically and dynamically. The aim of this work is to study cracking mechanisms on a particle level and to examine whether different failure mechanisms (i.e. adhesive and cohesive failure) can be used to explain the cracking behaviour of coating

layers. For the purpose, a new technique to produce SEM cross-sections has been applied. The technique uses an argon ion beam and the advantage is it does not require resin embedding. Earlier work by Ström et al. (2010) has shown that the sample preparation technique combined with high resolution microscope produces excellent SEM images where pigments, organic materials (such as binder) and pores can be distinguished from each other.

## Materials and Methods

### Sample preparation

For the trials, samples from previous works on cracking (Rättö, Hornatowska 2010a; 2010b) have been used. A copy paper, grammage 80 g/m<sup>2</sup> from Stora Enso, Finland, was used as a base substrate. A GCC pigment and a clay pigment were used in combination with one S/B latex and one starch binder. The GCC pigment was Hydrocarb 90 supplied from Omya, Switzerland, and the clay pigment was ND3090 supplied from Imerys, UK. The clay pigment had an average particle size of 0.51 µm with a shape factor of 27. The GCC pigment had an average particle size of 0.90 µm and was considered isometric. The latex was DL920 (Dow Chemicals, Switzerland), and the starch was supplied from Cargill, Germany. In coatings using only S/B latex as binder, 0.5 pph of CMC was added. The CMC was Finnfix 5 (CP Kelco, Finland).

The coating colours were mixed to a dry content of 65%. The coating colours consisted of four different pigment binder combinations given in *Table 1*. Samples containing 8 pph of binder were only analysed before creasing while samples containing 16 pph of binder were analysed before and after creasing.

The papers were coated in a laboratory coater from RK Print-Coat Instruments Ltd of Royston, England, model K-coater. A coat weight of 12 g/m<sup>2</sup> was applied and the papers were then oven-dried for 15 min at a temperature of 105°C. After drying, the papers were calendered in a laboratory calender from DT Paper Science, Finland. The line speed was 10 m/min and the line load 25 kN/m. The samples were printed in an offset laboratory printing press from IGT, Netherlands. A standard cyan ink, Toplith from Sun Chemicals, was used for the laboratory printing. All samples were printed in full tone. The printing was applied in order to measure the crack area in the previous works (Rättö, Hornatowska 2010a; 2010b) and has no particular function in this work.

The printed samples were creased in a creasing machine with two parallel lines, using a crease ruler with a ruler height of 23.25 µm. The creasing was performed at least 48 h after printing.

Table 1. Coating colour compositions.

Pigment	Binder system	Binder content
GCC	50% latex, 50% starch	8 pph
Clay	50% latex, 50% starch	8 pph
GCC	50% latex, 50% starch	16 pph
GCC	100 % latex	16 pph
Clay	50% latex, 50% starch	16 pph
Clay	100 % latex	16 pph

## Cross-sectional analysis

### Sample preparation

A cross-section polisher (CP) JEOL SE-09010 was used for all the cross-section polishing experiments. The cross-section polisher uses an ionized argon beam to polish the material of interest. For all the samples, the acceleration voltage of the argon ion beam was set to be 6kV, with a beam current of approximately 120  $\mu$ A. The cross-section obtained shows the original interior structure of the sample free from any extraneous contents and modification. A more detailed description of polishing technique can be found in an earlier work (Ström et al. 2010).

### SEM imaging

Low accelerating voltage SEM JSM-7401F was used to observe the cross-sections prepared by CP. Images were captured at 4500 x and 7000 x magnification. Landing voltage of 0.8 kV was applied to avoid the charging problem of the insulating material. The low landing voltage ensures that the image observed is surface information, since mostly secondary electrons are excited and detected at these low accelerating voltages. Meanwhile, the contrast created from different compositions can still be clearly seen because of the dependence of the secondary electron yield coefficient on atomic

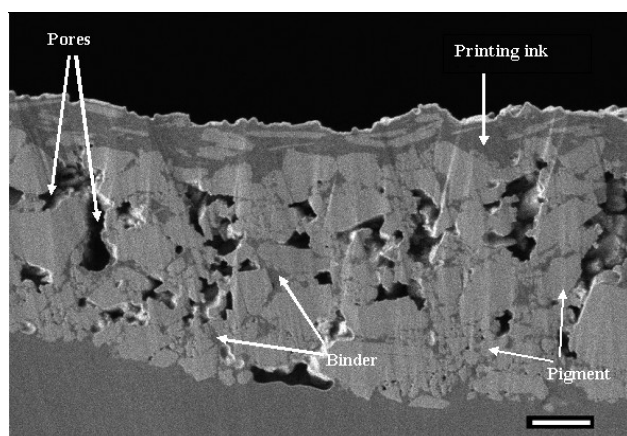


Fig 1. A SEM image illustrating the coating layer with a printing ink. The printing ink is located on the top of the coating and appeared as dark grey. The pigment particles of different sizes appear as light grey, with the binder appearing as grey. The black or unfilled areas between pigment particles are pores. A homogenous darker grey layer in the lower part of the image corresponds to a fibre wall and the white areas in the coating layer are edge effects. The scale bar is 1 $\mu$ m.

number, and the possible contribution from back-scattered electrons with high electron yield dependence on atomic number. The flatness of the cross-section made by CP reduces the edge effect and ensures that the contrast is obtained from the material composition only.

An example of one of the SEM images obtained by CP and its interpretation is shown in Fig 1. The identification of different components, i.e. ink, latex and pigments, is based on the results of Ström et al. (2010). Particles with a section size larger than 1  $\mu$ m are referred to as large particles, and particles with a section size smaller than 0.5  $\mu$ m are referred to as small particles.

## Results

Figs 2a-e show micrographs of the coated samples without cracks. The printing ink can be observed at the top of the coating layer on all the images. The left hand images show GCC-based coatings and the right hand images show the clay based coating. The binders, latex or starch, and the printing ink are represented as dark grey areas next to the pigment particles (light gray areas), and the pores are represented as black areas surrounded by the pigment particles and the binder.

At the lower binder contents, Figs 2a and 2b, the binder took up a very low volume. The GCC-based coating showed binder clusters around particles with a section size smaller than 0.5  $\mu$ m, while the clay base coating showed small areas of binder between the flat parts of the particles.

As the binder content increased, the binder enclosed the smaller particles (i.e. particles with a section size smaller than 0.5  $\mu$ m) of the GCC based coatings, Figs 2c and 2e. The binder also leaved large areas of the larger particles uncovered, creating large pores near the larger particles (i.e. particles with a section size larger than 1  $\mu$ m). These observations are consistent with observations made in an earlier work (Ström et al. 2010). The coatings containing starch showed a larger pore volume. This might be due to the higher density of starch compared to latex, or due to the possibility that part of the binder might have penetrated into the paper during the consolidation of the coating layer. The clay-based coatings with the higher binder content, Figs 2c and 2f, showed a similar pattern. The binder seemed to be concentrated into blocks around the smaller particles (i.e. particles with a section size smaller than 0.5 $\mu$ m), primarily at the flat sides of the particles. The starch containing coatings showed a larger pore volume, than the coatings with only latex, and the difference seemed to be larger for the clay-based coatings than the GCC-based coatings.

Figs 3 and 4 show micrographs of coated and

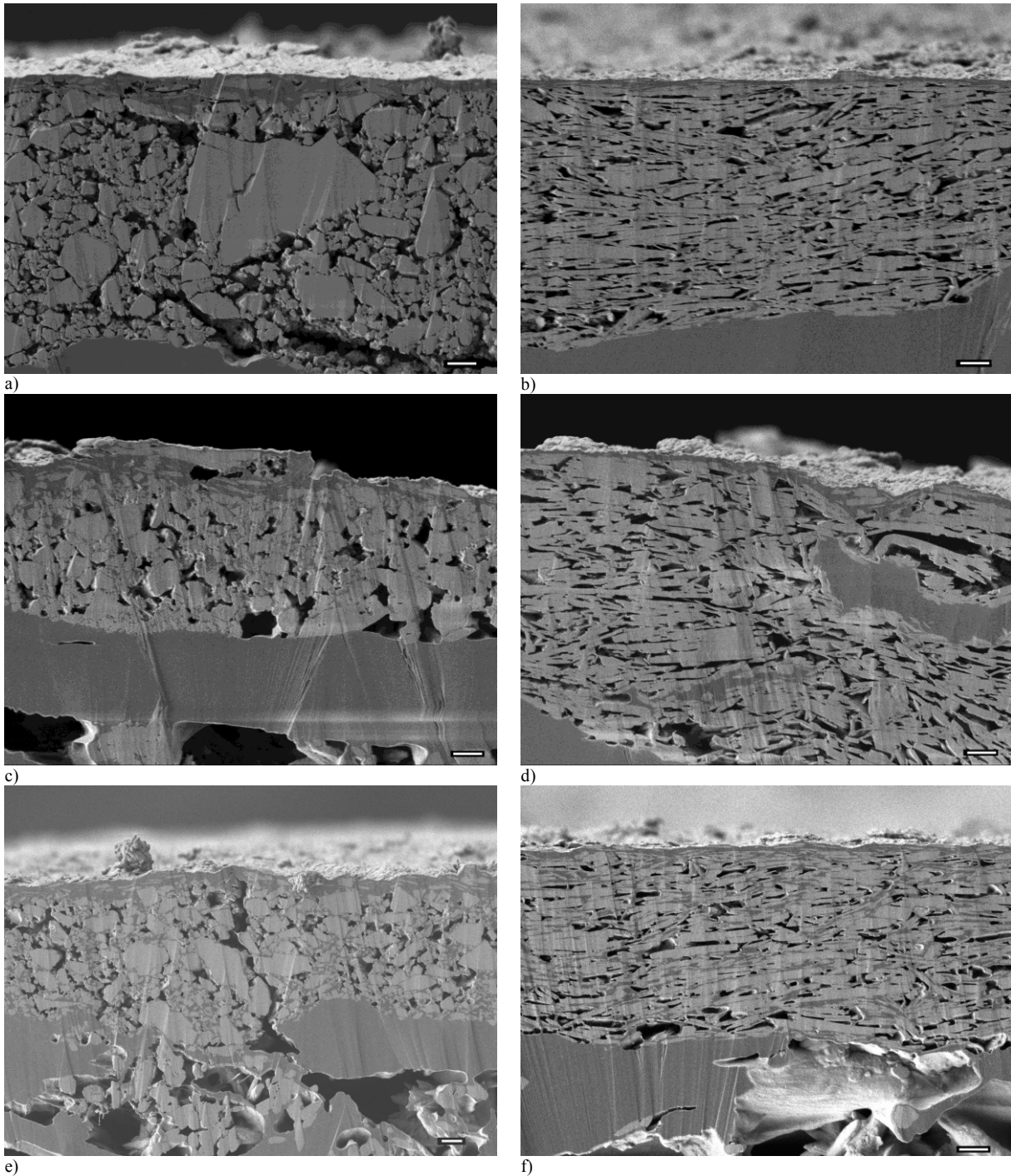


Fig 2. SEM micrographs of coated samples: a) represents GCC sample with 4 pph latex and 4 pph starch, b) clay with 4 pph latex and 4 pph starch, c) GCC with 8 pph latex and 8 pph starch, d) clay with 8 pph latex and 8 pph starch, e) GCC with 16 pph latex, and f) clay with 16 pph latex. The scale bars in the bottom right corner of each picture represent 1  $\mu\text{m}$ .

creased samples with a relatively high binder content, i.e. 16 pph. The GCC-based coating, *Figs 3a* and *3b*, exhibited cracks that went more or less straight through the coating layer, while the clay-based coating, *Figs 4a* and *4b* showed cracks that went at an angle along the coating layer thickness. The cracks were also observed near the base substrate, and seemed to follow the base line of the substrate. Cracks of the GCC-based coatings were usually wider at the surface of the coating layer indicating that the crack usually started from the

surface. The cracks of clay based coatings showed a wider crack at both the top of the coating layer and near the base paper. Cracks parallel to the base paper were also observed in the bulk of the coating layer. This indicates that cracks of clay based coatings could be initiated from the surface, in the bulk of the coating layer or near the interface between the coating layer and the base substrate. No significant difference in behaviour was observed between coatings containing starch and coatings containing only latex.

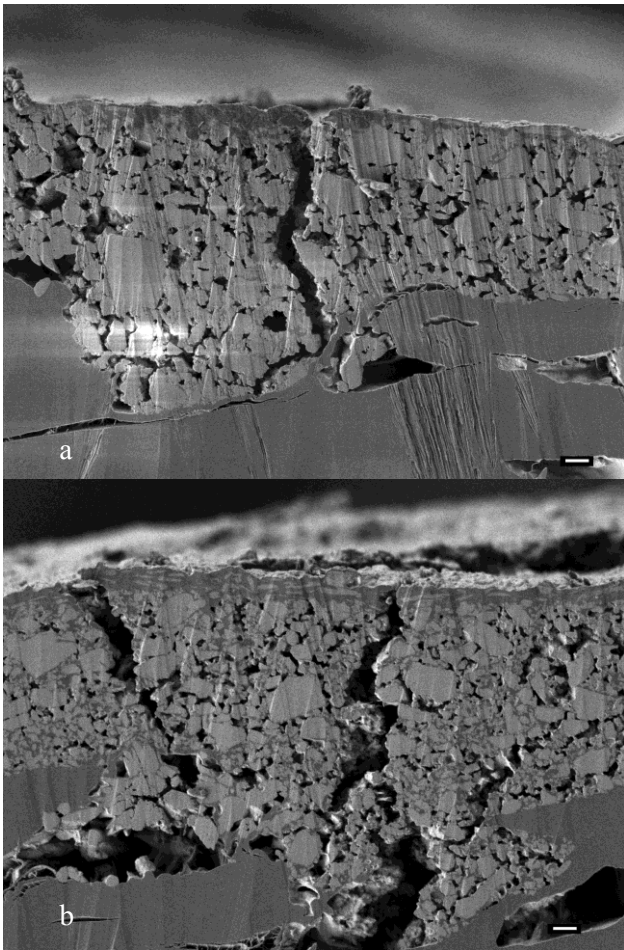


Fig 3. SEM micrographs of coated and creased samples: a) represents GCC with 8 pph latex and 8 pph starch, and b) GCC with 16 pph latex. The white bars at the bottom right corner of each picture represent 1  $\mu\text{m}$ .

*Figs 5 and 6* show cracks in coating layers on a particle level for the GCC- and clay-based coatings respectively. The crack in the GCC-based coating propagated adjacent to the larger particles (particles with a section size larger than 1  $\mu\text{m}$ ) of the coating layer. The crack line would follow the surface of the large particles, and continue more or less straight through the thickness direction of the coating layer. In the majority of cases, at least one of the crack surfaces was also free from binder. The free pigment surface was also usually the surfaces of large GCC particles. The same pattern was observed for the coatings containing starch, with at least one of the crack surfaces being free from binder and the crack seeming to propagate adjacent to the larger particles. The clay-based coatings (*Fig 6*) exhibited cracks that went through the coating layer at an angle in the thickness direction. The crack line followed the clay particle surfaces, leading to a gradual delamination of the coating layer along the direction of the clay particles. The initiation point of the crack in the coating layer was also harder to point out. The cracks could be initiated at the surface of the coating



Fig 4. SEM micrographs of coated and creased samples: a) represents clay with 8 pph latex and 8 pph starch, and b) clay with 16 pph latex. The white bars at the bottom right corner of each picture represent 1  $\mu\text{m}$ .

layer or near the base substrate. In the latter case, the cracks would usually propagate parallel to the base line of the substrate. Again, no significant difference in behaviour could be observed between the coatings containing starch and the coatings containing only latex.

## Discussion

Recent work (Ström et al 2010) has shown that relatively large pores are present in the coating layer, and the micrographs revealed, as was confirmed here, that the smaller pigment particles were surrounded by the binder. In the case of starch, there was a little less binder, possibly owing to the higher density of starch.

The local binder content around the larger particles was considerably smaller; the volumes surrounding these particles are quite probable points of crack initiation and crack propagation. This was also confirmed by the SEM micrographs of the creased coatings (*Figs 3- 6*), where the cracks seemed to follow a preferred path adjacent to the surface of the larger particles. No cracks at all could be observed

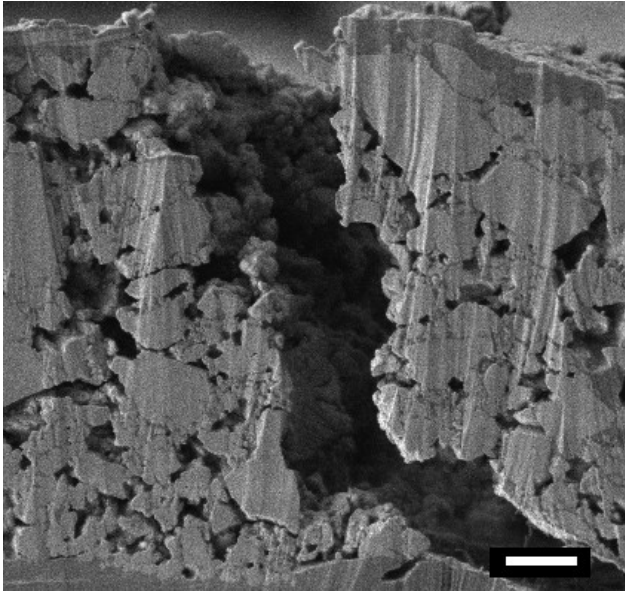


Fig 5. A SEM micrograph of coated and creased sample illustrating crack propagation in the GCC-based coating. The total binder content was 16 pph with 8 pph latex and 8 pph starch. A white arrow shows an area free of binder. The scale bar represents 1  $\mu\text{m}$ .

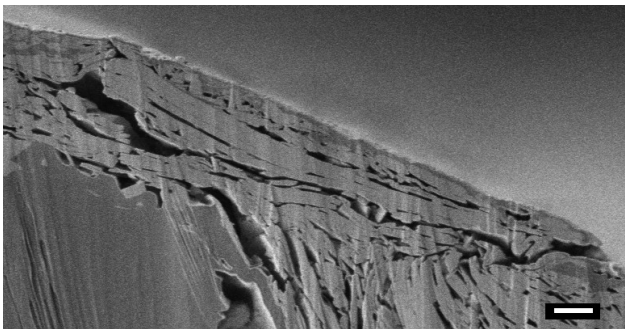


Fig 6. A SEM micrograph of coated and creased sample illustrating crack propagation of the clay-based coating at 4500x magnification. The total binder content was 16 pph with 8 pph latex and 8 pph starch. The scale bar represents 1  $\mu\text{m}$ .

through the parts of the coating layer with only small particles. This was probably due to the fact that these particles were surrounded by the binder, and the local strength of these volumes was stronger than the local strength of the volumes containing the large particles.

The coating layer itself is quite brittle. As a result, cracking through the coating layer is a fast process requiring only a low amount of strain energy before failure (Rättö, Hornatowka 2010a). It has also been suggested by Alam and Toivakka (2010) that the mechanical behaviour depends on the interaction between the pigment particles and the binder. A more brittle behaviour would be obtained if the break were adhesive (i.e. if the break is between the pigment particle surface and the binder) rather than cohesive (i.e. the break is within the binder). A cohesive break would show two crack areas containing binder, while at least one of the crack areas would exhibit a pigment surface for an adhesive break. The fact that almost all the crack

surfaces showed at least one pigment surface indicates that cracking was due to adhesive failure and this, together with the simulation results of Alam and Toivakka (2010), would explain the brittle behaviour observed by Rättö and Hornatowska (2010a). One should on the other hand be aware of the possibility of that the ink vehicle penetration might influence the mechanical properties of the binder. It shall here be mentioned that this study has been on comparable basis and all the creased samples studied had been subjected to the same treatment. Most products that are creased and folded are usually printed before these operations anyway, and the results here would thus be more realistic than if the study was performed on non-printed samples.

The micrographs presented here also confirmed earlier results (Rättö, Hornatowska 2010b), but the information here is on a particle level. It was quite obvious that the isometric particle shape of the GCC coatings would result in nearly isotropic material behaviour, while the flat pigment particles of the clay pigment would result in strong in-plane properties and weak out-of-plane and weak shear properties. This will mostly influence the failure process of the coating layer. The break through the GCC coatings would show a crack almost straight through the coating layer. The clay particles, on the other hand, would show cracks that would go at the angle of the coating layer, where the site of failure would seem to be between the basal surfaces of clay particles. The clay-based coatings also showed cracks that were near and parallel to the base substrate. The different cracking mechanisms can be explained, to some extent, by beam theory, which can be found in basic literature on sandwich construction (e.g. Zenkert 1992, Vinston 2006) or from numerical simulations found in literature (Nygårds et al. 2009).

The flexural rigidity of a sandwich beam consisting of a core layer (e.g. base paper) surrounded by two outer layers (e.g. coating layers) can be described as:

$$D = \int E \cdot z^2 dA = b \cdot \left\{ \frac{E_f \cdot t_f^3}{6} + \frac{E_f \cdot t_f \cdot d^2}{2} + \frac{E_c \cdot t_c^3}{12} \right\} \quad [1]$$

where  $b$  is the width of the sample,  $E_f$  and  $t_f$  are the elastic modulus and thickness of the of the outer layers (i.e. the coating layers),  $E_c$  and  $t_c$  are the elastic modulus and thickness of the of the core layer (i.e. the base substrate) and  $d$  is half the thickness of the sandwich beam. If the beam is subjected to a load, this load will be supported in the beam by a transverse force,  $T$ , and a momentum,  $M$ .

The momentum will give rise to an in-plane normal stress that depends on the distance from the symmetry line of the beam,  $z$ . The stress in the outer layer is described by:

$$\sigma_f = \frac{M \cdot z \cdot E_f}{D} \quad [2]$$

and the stress in the core is described by:

$$\sigma_c = \frac{M \cdot z \cdot E_c}{D} \quad [3]$$

The transverse force would give rise to a shear force in both the outer layer:

$$\tau_f = \frac{T}{D} \cdot \frac{E_f}{2} \left[ \frac{t_c^2}{4} + t_c \cdot t_f + t_f^2 - z^2 \right] \quad [4]$$

and in the core:

$$\tau_c = \frac{T}{D} \left[ \frac{E_f \cdot t_f \cdot d}{2} + \frac{E_c}{2} \cdot \left( \frac{t_c^2}{4} - z^2 \right) \right] \quad [5]$$

The normal stress and the shear stress as a function of the position in the thickness direction,  $z$ , are plotted in *Figs 7a* and *7b*.

The shear force (*Fig 7b*) shows a maximum in the middle of the core and would decrease towards the top and bottom of the sandwich. The maximum shear force in the outer layer would thus be at the interface between the top layer and the core layer. For a coated paper, this would be in the interface between the coating layer and the base substrate.

The maximum tensile force (*Fig 7a*) is reached at the top of the outer layer, and this is one probable explanation of why the cracks seem to start at the top of the coating layer and propagate straight through the thickness direction for the GCC-based coatings. Clay based coatings are generally more resistant to in-plane tensile forces (Lepoutre, Rigdahl 1989, Husband et al. 2007) at the expense of the out-of-plane and shear strength.

The shear forces would normally not be of importance for failure in beam mechanics, but in some circumstances might be responsible for failure in the core material or near the interface. Such circumstances in this case include weak shear

strength of an outer layer. The layered structure of clay based coatings is probably quite weak when exposed to shear forces (Rättö 2006) and the shear stresses during the creasing operation are probably sufficient to cause a failure and delamination. The clay based coating layers did not however necessarily delaminate at the interface, but quite often in the bulk of the coating layer. Here, the fibres of the base substrate may have reinforced the coating layer.

It should also be mentioned that creasing shows a more complicated loading case than described by beam theory. Numerical simulations of creasing of board performed by Nygård et al. (2009) exposed both shear stresses and out-of-plane tensile stresses at the surface of the board. The loading case during creasing may therefore quite probably cause delamination of layered structures such as clay based coatings.

## Conclusions

The binder gathered around the small pigment particles leaving large pores around the larger pigment particles in both latex and starch containing coatings. This would result in a lower local strength of volumes with larger pigment particles. Consequently, cracking propagated adjacent to the surface of larger pigment particles. The crack surfaces also showed at least one surface free from binder and failure would thus be in the interface area between the binder and the pigment particle. Cracking in coating layers would thus be due to adhesive failure rather than cohesive failure.

GCC based coatings showed cracks that went through the coating layer thickness while clay based coatings showed cracks that went in an angle to the thickness direction or parallel with the base substrate. Since beam theory and numerical simulations have shown that creasing result in shear stresses and out of plane stresses, the delamination of clay is probably due to the weak shear strength and weak out-of-plane tensile strength of the coating layer combined with the loading case.

## Acknowledgements

The author expresses their abundant thanks to RISE for financial support, and to the Knut and Alice Wallenberg Foundation for its support to EM Centre at Department of Materials and Environmental Chemistry, Stockholm University.

The authors also wishes to thank Prof. Göran Ström for scientific advice, Dr Christophe Barbier of Karlstad University for his valuable comments and Kenneth Blomquist, Blomquist & Partner for linguistic revision of the manuscript, Mrs Jolanta Borg for preparing the laboratory-coated papers and performing the crack area measurements, Mrs Anni Hagberg for performing the laboratory printing of the samples, Mr Birger Edholm for performing the creasing, and Mr Hans Christiansson for programming the customised software package for the crack area measurements.

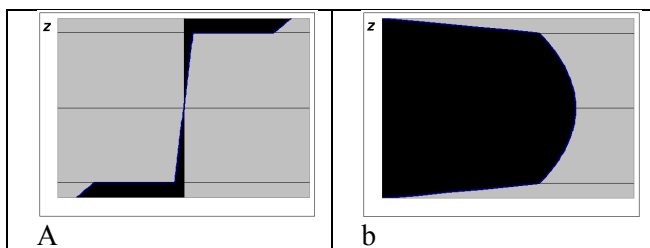


Fig 7. a) The normal stress plotted through the thickness direction,  $z$ , of a sandwich beam consisting of a soft core layer surrounded by two stiff outer layers, b) The shear stress plotted through the thickness direction,  $z$ , for the same beam as in a).

---

## Literature

- Alam P., Toivakka M., Carlsson R., Salminen P., Sandås S.** (2009): "Balancing between fold-crack resistance and stiffness", *J. of Composite Mat.*, 43(11), 1265-1283.
- Alam P., Toivakka M.** (2010): "Cohesive versus adhesive mechanisms of failure in paper coatings – a modelling approach", *TAPPI 11<sup>th</sup> Adv. Coat. Fund. Symp.*, Oct 11-13, 2010, Munich, Germany.
- Alam P., Xu Q., Toivakka M., Hämäläinen H., Syrjälä S.** (2007): "The elastic modulus of paper coating in tension and compression", *TAPPI Coat and Graph. Arts Conf.*, 22-25 Apr. 2007, Miami, FL, USA, 2007.
- Barbier C., Larsson P. L., Östlund S.** (2002): "Experimental investigation of damage at folding of coated papers", *Nord. Pulp Pap. Res. J.*, 17(1), 34-38.
- Barbier C., Larsson P. L., Östlund S.** (2004): "Numerical investigation of folding of coated papers", *Composite Struct.*, vol. 67, 383-394.
- Colley J.** (1982a): "The crease cracking tendency of light-weight coated magazine papers part I: development of test method", *Appita*, 35(4), 299-302.
- Colley J.** (1982b): "The crease cracking tendency of light-weight coated magazine papers part II: factors affecting crease cracking tendency", *Appita*, 35(6), 499-504.
- Dia J.S., Cannella F.** (2008): "Stiffness Characteristics of Carton Folds for Packaging", *Trans. ASME, J. of Mech. Design*, vol. 130, 022305-1 – 022305-2.
- Guyot C, Bacquet, G., Schwob J. M.** (1992): "Folding resistance of magazine papers", *Proc. Tappi Coating Conf.*, Orlando, FL, USA, 17-20 May, 255-268.
- Husband, J. C., Preston, J. S., Gate, L. F., Storer, A. and Creaton, P.** (2007): "The influence of pigment particle shape on the in-plane tensile strength properties of kaolin-based coating layers", *Tappi J.*, 5(12), 3-8.
- Husband J.C., Gate L.F., Norouzi N., Blair D.S.** (2009): "The Influence of Kaolin Shape Factor on the Stiffness of Coated Paper", *Tappi J.*, June 2009, 12 – 17.
- Kan C.S., Kim L.H., Lee D.I., van Gilder R.L.** (1997): "Viscoelastic properties of paper coatings: Relationship between coating structure – viscoelasticity and end-use performance", *Tappi J.*, 80(5), 191-201.
- Jopson R.N., Towers K.** (1995): "Improving fold quality in coated papers and boards – the relationship between base stock and coating", *Tappi Coating Conf.*, Atlanta, USA, 459-477.
- LePoutre P., Rigdahl, M.** (1989): "Analysis of the effect of porosity and pigment shape on the stiffness of coating layers", *Mat. Sci.*, 24, 2971-2974.
- Nygårds M., Just M., Tryding J.** (2009): "Experimental and numerical studies of creasing of paperboard", *Int. J. of Solids and Struct.*, 46, 2493-2505.
- Prall K.M., Shaler S.M., LePoutre P.F.** (2000): "Pigmented latex coatings: Microstructure and viscoelastic properties", *Nord. Pulp Pap. Res. J.*, 15(5), 564-571.
- Rättö P.** (2004): "Mechanical properties of coating layers", *J. Pulp Pap. Sci.*, 30(12), 335-340.
- Rättö P.** (2006): "Pressure distribution on coated papers", *Prog. Paper Phy. Sem.*, Miami University, Oxford, Ohio, USA, Oct 1-5, 2006.
- Rättö P., Hornatowska J.** (2010a): "Dynamic aspects of crack development in coating layers", *TAPPI 11<sup>th</sup> Adv. Coat. Fund. Symp.*, Oct 11-13, 2010, Munich, Germany.
- Rättö P., Hornatowska J.** (2010b): "The influence of coating colour composition on the crack area after creasing", *Nord Pulp Pap Res. J.*, 25(4), 488-494.
- Salminen P., Carlsson R., Sandås S., Toivakka M., Alam P., Roper J.** (2008a): "Combined modeling and experimental studies to optimize the balance between fold crack resistance and stiffness for multilayered paper coatings - part 1: Introduction and modeling studies", *In Proc. TAPPI Coat and Graph. Arts Conf.*, TAPPI Press, Atlanta, USA, 2008
- Salminen P., Carlsson R., Sandås S., Toivakka M., Alam P., Roper R.** (2008b): "Combined modeling and experimental studies to optimize the balance between fold crack resistance and stiffness for multilayered paper coatings - part 2: Pilot coater experimental studies", *Proc. TAPPI Coat. and Graph. Arts Conf.*, TAPPI Press, Atlanta, USA, 2008.
- Ström G., Hornatowska J., Changhong X., Terasaki O.** (2010): "A novel SEM cross-section analysis of paper coating for separation of latex from void volume", *Nord. Pulp Pap. Res. J.*, 25(1), 107-113.
- Toivakka M., Bousfiled D.** (2001): "Modeling of coating layer mechanical properties", *Proc. TAPPI Advanced Coating Fund. Symp.*, 197-211.
- Wikström M., Mäkelä P., Rigdahl M.** (2000): "Influence of temperature and type of latex on the out-of-plane compression behaviour of coating layers", *Tappi J.*, vol 83, no 8, 92.
- Vinston J.R.** (2006): "Plate and Panel Structures of Isotropic, Composite and Piezoelectric Materials, Including Sandwich Construction", *Electronic resource*, Springer, 2005.
- Zenkert D.** (1992): "An introduction to sandwich construction", *Paper 92-5*, ISSN 0280-4646, Dept. of Lightweight Structures, Swedish Royal Institute of Technology (KTH), 1992.

Manuscript received May 17, 2011

Accepted August 25, 2011